Journal of Bio- and Tribo-Corrosion (2019) 5:42
https://doi.org/10.1007/s40735-019-0237-5

Inhibition of Carbon Steel Corrosion in HCl and H_2SO_4 Solutions by Ethyl 2-Cyano-2-(1,3-dithian-2-ylidene) Acetate

Abdelali Fiala[1] · Wafia Boukhedena[2] · Salah Eddine Lemallem[1] · Hayet Brahim Ladouani[1] · Hamza Allal[3]

Received: 16 January 2019 / Revised: 14 March 2019 / Accepted: 18 March 2019 / Published online: 28 March 2019

Abstract
The adsorption behaviour of Ethyl 2-cyano-2-(1,3-dithian-2-ylidene) acetate (ECDYA) on carbon steel and its inhibitive action on corrosion in 1 M HCl and 0.5 M H_2SO_4 aqueous solutions were examined using different corrosion evaluation methods, such as weight loss, potentiodynamic polarisation and electrochemical impedance spectroscopy. The results obtained showed that the inhibitory character of this product increases with the concentration but this character is inversely related to the temperature. Tafel curves have revealed that this compound (ECDYA) possesses the indices of a mixed inhibitor. The inhibiting effect of this compound was interpreted through its adsorption on the metal surface. The Langmuir isotherm adequately describes the process of adsorption of the ECDYA molecules on the surface of the steel in this medium. The experimental results revealed that ECDYA restrains the corrosion reaction in both acidic environments, the inhibition efficiency being stronger in H_2SO_4 than in HCl. The discussion of kinetic and thermodynamic parameters such as activation energy, enthalpy, entropy and adsorption free energy has also been the subject of this work. Quantum chemical parameters were calculated and discussed.

Keywords Corrosion inhibitor · Carbon steel · Acidic media · Ethyl 2-cyano-2-(1,3-dithian- 2-ylidene) acetate · Density functional theory

1 Introduction

Owing to its low cost and good availability, carbon steel (CS) has been extensively used for different purposes in a wide range of industrial applications such as automotive, transportation and several other fields. Furthermore, hydrochloric and sulphuric acids are widely used for pickling and de-scaling of carbon steel, promoting the acceleration of metallic corrosion with potential adverse effects on the ecological balance and in the economic field, namely in term of repair, replacement and products losses [1, 2]. Different organic compounds have been reported to be as effective corrosion inhibitors during acidization in industrial cleaning processes [3–6]. Various organic compounds containing polar functions in their structures have been reported as being effective corrosion inhibitors for CS in acidic solutions [7–12]. Researches concerning corrosion processes and their inhibition by organic compounds have been conducted recently, and a number of interesting papers have been published. Over the last few decades, many new inhibitors were synthesised. In principle, organic inhibitors prevent metal corrosion by interacting with the metal surface via adsorption thru the donor atoms, π-orbital, electron density and the electronic structure of the molecule [13–18]. These inhibitors are usually adsorbed on the metal surface via formation of a coordinate covalent bond (chemical adsorption) or electrostatic interaction between the metal and inhibitor (physical adsorption) [19]. The chemical structure of the inhibitors, the type of aggressive electrolyte, the nature and the charge of the surface of the metal has a considerable impact on this phenomenon. The compounds that contain both nitrogen and sulphur exhibit high inhibitory efficacy compared to those containing only nitrogen or sulphur [3, 20–22]. It is therefore established that organic compounds

✉ Abdelali Fiala
abdelfiala1@umc.edu.dz

[1] Chemistry Research Unit Environmental and Structural Molecular, CHEMS. Mentouri Brothers Constantine 1 University, 25000 Constantine, Algeria

[2] Department of Science Matter, Larbi Tebessi University, 12000 Tebessa, Algeria

[3] Department of Technology, Faculty of Technology, 20 August 1955 Skikda University, 21000 Skikda, Algeria

having a molecular structure containing nitrogen, oxygen, phosphorus and sulphur and/or π-electron of double or triple bonds, are usually used in the protection against corrosion of metals and their alloys in acidic environments [23]. Therefore, it seemed interesting to us to synthesise a new compound belonging to ketene dithioacetals derivatives, ECDYA, having a structure presenting this advantage, and to study, in its presence and in its absence, the behaviour of carbon steel in 1.0 M HCl and 0.5 M H_2SO_4 aqueous solutions. Moreover, some compounds of the same family of this compound gave satisfactory results in inhibiting the corrosion of copper in 3 M HNO_3 [24]. The study has been carried out using weight loss and potentiodynamic polarisation measurements along with electrochemical impedance spectroscopy (EIS) and scanning electron microscopy (SEM) investigations. In other hand, the local chemical reactivity of this compound was performed using the density functional theory (DFT) via the CAM-B3LYP method [25].

2 Materials and Experimental Methods

2.1 Materials

2.1.1 Inhibitor

Ethyl 2-cyano-2-(1,3-dithian-2-ylidene) acetate (ECDYA) was synthesised by first mixing K_2CO_3 (42 g, 0.3 mol) and ethyl 2-cyanoacetate, an active methylene compound, (0.1 mol) in 50 mL of DMF and placing the mixture under magnetic stirring. 9 mL (0.15 mol) of carbon disulphide were then added in one go at room temperature. The stirring was maintained for 10 min before starting the dropwise addition of the dielectrophilic reagent, 1,3-dibromopropane, (0.12 mol), an operation that stretches over 20 min. After 7 h stirring at room temperature, 500 mL of ice water were added to the reaction mixture. The solution was filtered thru a paper filter to isolate the precipitate that formed. The latter was recovered, dried, purified by recrystallisation from ethanol and used in the experiments in the concentration range [5×10^{-6}; 10^{-3}] mol/L [24]. The details of its crystalline structure are given in a previous publication [26]. Figure 1 shows that the structural formula of ECDYA. It exhibited the following characteristics.

This product is recovered in the form of a yellow precipitate. Its molar mass is M = 229 g/mol. Yield: 93%; M.P = 95 °C. FT-IR (FT-IR spectra of ECDYA obtained for its solid state, υ (cm^{-1})): 1700(C=O), 1246–1004(C–O (ester)), 2206(C≡N), 1437(C=C). ^{1}H NMR (($CDCl_3$), δ(ppm), 250 MHz)): 1.35 (t, 3H, CH_3–CH_2), 2.35 (p, 2H, CH_2), 2.95–3.25 (m, 4H, $2CH_2S$), 4.30 (q, 2H, CH_2O). The mass spectroscopy analysis revels that the inhibitor produced fragment ions m/z 229. ^{13}C NMR ($CDCl_3$, δ(ppm), 250 MHz: 14.22(s,$\underline{C}H_3$–CH_2–O), 23.36(s, S–CH_2–$\underline{C}H_2$–CH_2–S), 28.99(s, S–$\underline{C}H_2$–CH_2–$\underline{C}H_2$–S), 61.26(s, CH_3–$\underline{C}H_2$), 76.69(s,O=C–$\underline{C}$=C), 120.55(s, $\underline{C}$N), 165.56(s, O–$\underline{C}$=O), 180.7(s, C=$\underline{C}S_2$).

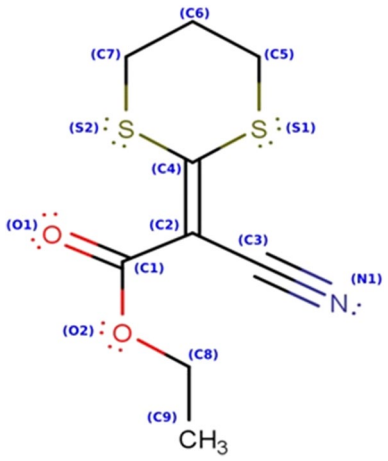

Fig. 1 Structure formula of Ethyl 2-cyano-2-(1,3-dithian-2-ylidene) acetate (ECDYA)

2.1.2 Specimen

Corrosion tests were performed on carbon steel specimens of the following chemical composition (wt%): C 0.09%, Si 0.05%, Mn 0.13%, S 0.24%, P 0.24% and Fe balance. For the gravimetric and electrochemical measurements, pre-treatment of the surface of specimens was carried out by mechanically grinding with 500, 800, 1000 and 1200 grades of emery papers. Then, they were washed with distilled water, degreased with acetone and dried at room temperature before use in the experiments. In the gravimetric measurements, the carbon steel samples were cubic (1 cm × 1 cm × 1 cm); those used in electrochemical measurements (PC and EIS) were protected by the epoxy resin leaving a working surface equal to 0.5 cm^2.

2.1.3 Electrolyte Medium

The aggressive solutions were 1 M HCl [prepared by dilution of 37% w/w HCl (Merck)] and 0.5 M H_2SO_4 [prepared by dilution of 98% w/w H_2SO_4 (Merck)] with bi-distilled water. All tests were performed in the aerated medium at different temperatures (293 K, 303 K, 313 K, 323 K and 333 K).

2.2 Methods

2.2.1 Weight Loss Measurements

Gravimetric experiments were carried out in a glass vessel. The specimens were prepared as described above and then weighed. The test pieces were immersed in 100 mL of 1 M HCl and 0.5 M H_2SO_4 with various concentrations of inhibitor. After 5 h, three test pieces were taken out of the test solution, washed, dried and weighed again. The mean value of weight loss for each set of data with the corresponding standard deviation is reported here. The corrosion rate (V_{corr}) was calculated from the weight loss data according to Eq. (1) [9]:

$$V_{corr} = \Delta W / St \tag{1}$$

where ΔW is the average weight loss (mg), S is the total surface area of the specimen (cm^2) and t is the immersion period (5 h). The inhibitory efficiency ($IE_w\%$), as well as the surface coverage (θ), were determined using the following equations.

$$\theta = \frac{V_{corr-} V'_{corr}}{V_{corr}} \tag{2}$$

$$IE_w(\%) = \left(\frac{V_{corr-} V'_{corr}}{V_{corr}}\right) \times 100 \tag{3}$$

where, V_{corr} and V'_{corr} are the corrosion rates of carbon steel respectively in the absence and in the presence of inhibitor.

2.2.2 Electrochemical Measurements

A Voltalab-PGZ 301 potentiostat controlled by a computer using Voltamaster 4 software was used for electrochemical measurements. The cell used was a three-electrode Pyrex glass cell, with CS as the working electrode (WE), SCE as the reference electrode (RE) and Pt as the counter electrode (CE). Before each measurement, a stationary state of the system was achieved by immersing a freshly polished electrode in the test solution at open circuit potential for 20 min.

Potentiodynamic polarisation curves for different concentrations of the inhibitor were obtained with a scan rate of 0.5 mV s^{-1}, starting from a cathodic potential of −250 mV to an anodic potential of +250 mV relative to the E_{ocp}. Measurements by electrochemical impedance spectroscopy are carried out at the open circuit potential, OCP, over a frequency range from 100 kHz to 10 mHz with a perturbation using a signal of equal amplitude at 10 mV. Every potential esteem was estimated in reference to immersed calomel electrode (SCE). Each experiment was repeated at least three times to check the repeatability.

2.2.3 Surface Analysis

The surface morphology of the samples exposed to acid solutions without and with containing 10^{-3} M of ECDYA was studied by a scanning electron microscope model JEOL JSM-6360 LV. The SEM analysis was done after 3 h immersion of all samples at 298 K.

2.2.4 DFT Computational Details

The DFT quantum chemical calculations were performed with the ORCA 4.0.1.2 computational package [27, 28], using the CAM-B3LYP/def2-TZVPP level of the theory [29]. All calculated compounds were initially prepared and minimised by using Avogadro programme [30], applying MMFF94 s force field.

According to Koopman's theorem [31], first ionisation energy (I) and electron affinity (A) is approximately equal (with the minus sign) to the highest occupied molecular orbital energy (HOMO) and the lowest unoccupied molecular orbital energy (LUMO), respectively.

$$I = -E_{HOMO} \tag{4}$$

$$A = -E_{LUMO} \tag{5}$$

The HOMO and LUMO are more closely associated with the ability of a molecule to donate and accept electrons, respectively. Moreover, the difference of E_{HOMO} and E_{LUMO}, termed the band gap (ΔE_{gap}), is important parameters to characterise the reactivity of a chemical species. Lower values of the energy difference ΔE_{gap} will cause higher inhibition efficiency because the energy to remove an electron from the last occupied orbital will be low [32].

$$\Delta E_{Gap} = E_{LUMO} - E_{LUMO} \tag{6}$$

The electronegativity (χ) and the global hardness (η) [33] are based respectively on the first and second partial derivatives of the energy (E) relative to the number of electrons (N) and the external potential v (r).), using the following equations:

$$\chi = -\pi = -\left(\frac{\partial E}{\partial N}\right)_{v(r)} \tag{7}$$

$$\eta = -\left(\frac{\partial^2 E}{\partial N^2}\right)_{v(r)} \tag{8}$$

where the first equality in the Eq. (7) corresponds to the chemical potential (π), identified as negative of the electronegativity. The equations resulting from the finite difference method [34], with which the calculation of μ, η and π can be given as follows:

$$\chi = \frac{I + A}{2} \tag{9}$$

$$\eta = \frac{I - A}{2} \tag{10}$$

Global softness (σ) is defined as the inverse of the global hardness [35]:

$$\sigma = \frac{1}{\eta} = \frac{2}{I - A} \tag{11}$$

Fukui function $f(\vec{r})$ is defined as the derivative of the electronic density $\rho(\vec{r})$ relative to the number of electrons N at a constant external potential $v(\vec{r})$ [36]:

$$f(\vec{r}) = \left(\frac{\partial \rho(\vec{r})}{\partial N} \right)_{v(\vec{r})} \tag{12}$$

Fukui functions [37] were calculated using the following equations.

$$f_k^+ = q_k(N+1) - q_k(N) \text{(nucleophilic attack)} \tag{13}$$

$$f_k^- = q_k(N) - q_k(N-1) \text{(electrophilic attack)} \tag{14}$$

where $q_k(N+1)$, $q_k(N)$ and $q_k(N-1)$ are the charges of the atoms on the systems with $N+1$, N, and $N-1$ electrons respectively. Higher f_k^+ values for an atom (k) indicate a preference towards a nucleophilic attack, while higher f_k^- values indicate a preference for an electrophilic attack on this atom.

In order to facilitate the comparison between the possible sites for nucleophilic and electrophilic attacks on any atom k, we have calculated (Δf_k) which corresponds to the difference ($f_k^+ - f_k^-$), because if $\Delta f > 0$, then the site is favourable for a nucleophilic attack, whereas if $\Delta f < 0$, then the site is favourable for an electrophilic attack [32].

3 Results and Discussion

3.1 Weight Loss Measurements

The corrosion rate (V_{corr}), the surface coverage (θ) and the inhibition efficiency ($IE_w\%$) obtained from weight loss measurements of steel specimens after 5 h exposure to 1 M HCl and 0.5 M H_2SO_4 solutions with and without the addition of various concentrations of the investigated inhibitor (ECDYA) at different temperatures were calculated. The resulting data are gathered in Table 1. The effect of this inhibitor on the corrosion of carbon steel in these two media was monitored for 24 h by this method. By way of example, the inhibitory efficacy reached a value equal to 80.9% for 5 h of exposure to the aggressive 1 M HCl medium at a concentration of 10^{-3} mol L^{-1} at 293 K and at 97.9% in 0.5 M H_2SO_4 under the same conditions. This efficiency became equal to 77.3% for a 24 h exposure time in 1 M HCl and 89.1% in 0.5 M H_2SO_4 under the same conditions as previously.

Examination of the data in Table 1 reveals that the addition of ECDYA decreases the corrosion rate of carbon steel, while inhibition efficiency ($IE_W\%$) and surface coverage (θ) increase with increasing inhibitor concentration at all temperatures. At 10^{-3} M, ECDYA exhibits maximum inhibition efficiency (80.9% in 1 M HCl and 97.9% in 0.5 M H_2SO_4) at 293 K. This concentration represents the efficient inhibitive ability. This can be due to the inhibitor molecules act by adsorption on the metal surface [38]. Generally, the efficiency of an organic substance acting as a metallic corrosion inhibitor depends on the chemical structure and the concentration of the inhibitor, the metal nature and other experimental conditions, such as medium temperature [39]. The plot of V_{corr} versus concentration of ECDYA at 293 K (none showed) clearly indicates that corrosion rate was reduced in the presence of ECDYA in comparison to the blank in both acidic media. The fact that the metal specimen manifests higher corrosion susceptibility in 1 M HCl is evidence that the anions of the acids which influence the corrosion process in different ways. It is evident too from Table 1 that the inhibition efficiency increases with increasing ECDYA concentration but decreases with increasing the temperature (293–323 K), both in 1 M HCl and 0.5 M H_2SO_4 solutions. This may be explained by a regress of adsorption-induced by the temperature rise [40], a phenomenon that is frequent in physisorption, and an increased rate of dissolution process of carbon steel.

3.2 Potentiodynamic Polarisation Measurements

Potentiodynamic polarisation measurements were carried out to gain insight into the kind of corrosion protection supplied by ECDYA, i.e. to determine whether inhibition is anodic, cathodic or a mixed type, and its effect on the kinetics of the anodic and cathodic reactions [41, 42]. The inhibitory efficiency ($IE\%$) calculated according to Eq. (15) [43].

$$IE_p\% = \left(\frac{i_{corr}^0 - i_{corr}^{inh}}{i_{corr}^0} \right) \times 100 \tag{15}$$

where i_{corr}^0 and i_{corr}^{inh} are the corrosion current densities in the absence and the presence of a defined concentration of inhibitor, respectively. The kinetic parameters, namely the corrosion current density (I_{corr}), the corrosion potential (E_{corr}), the cathodic Tafel slope (β_c) and the anodic Tafel slope (β_a) are summarised in Table 2. Figure 2a, b shows the cathodic and anodic Tafel polarisation curves of carbon steel

Table 1 Mass loss data for carbon steel immersed in 1 M HCl and 0.5 M H_2SO_4 solutions with and without various concentrations of ECDYA in the temperature range of 293 K to 323 K

T (K)	C (M)	1 M HCl			0.5 M H_2SO_4		
		V_{corr} (mg cm^{-2} h^{-1})	θ	IE_w (%)	V_{corr} (mg cm^{-2} h^{-1})	θ	IE_w (%)
293	Blank	1.856	–	–	0.307	–	–
	5×10^{-6}	0.906	0.512	51.2	0.079	0.743	74.3
	1×10^{-5}	0.627	0.662	66.2	0.054	0.824	82.4
	5×10^{-5}	0.591	0.682	68.2	0.047	0.847	84.7
	1×10^{-4}	0.491	0.736	73.6	0.035	0.886	88.6
	5×10^{-4}	0.448	0.759	75.9	0.019	0.938	93.8
	1×10^{-3}	0.354	0.809	80.9	0.006	0.981	98.1
303	Blank	2.493	–	–	0.440	–	–
	5×10^{-6}	1.719	0.311	31.1	0.121	0.725	72.5
	1×10^{-5}	1.620	0.350	35.0	0.091	0.793	79.3
	5×10^{-5}	1.371	0.450	45.0	0.081	0.816	81.6
	1×10^{-4}	1.121	0.550	55.0	0.076	0.827	82.7
	5×10^{-4}	1.022	0.589	58.9	0.073	0.834	83.4
	1×10^{-3}	0.947	0.620	62.0	0.034	0.923	92.3
313	Blank	7.521	–	–	0.725	–	–
	5×10^{-6}	5.892	0.217	21.7	0.294	0.595	59.5
	1×10^{-5}	5.295	0.296	29.6	0.255	0.648	64.8
	5×10^{-5}	4.974	0.339	33.9	0.219	0.698	69.8
	1×10^{-4}	4.205	0.441	44.1	0.127	0.825	82.5
	5×10^{-4}	3.244	0.569	56.9	0.111	0.847	84.7
	1×10^{-3}	3.190	0.576	57.6	0.079	0.891	89.1
323	Blank	13.620	–	–	1.596	–	–
	5×10^{-6}	11.190	0.178	17.8	0.921	0.423	42.3
	1×10^{-5}	9.850	0.277	27.7	0.804	0.496	49.6
	5×10^{-5}	9.336	0.315	31.5	0.681	0.573	57.3
	1×10^{-4}	8.501	0.376	37.6	0.648	0.594	59.4
	5×10^{-4}	7.433	0.454	45.4	0.462	0.711	71.1
	1×10^{-3}	6.930	0.491	49.1	0.414	0.741	74.1

Table 2 Results obtained by Tafel extrapolation of carbon steel immersed in 0.5 M H_2SO_4 and 1 M HCl solutions with and without various concentrations of ECDYA at 293 K

Acid solutions	C_{inh} (M)	$-E_{corr}$ (mV vs. SCE)	$-\beta_c$ (mV dec^{-1})	β_a (mV dec^{-1})	i_{corr} (mA cm^{-2})	IE (%)
0.5 M H_2SO_4	0	500.6	100.0	94.3	1.122	/
	5×10^{-6}	467.3	157.7	150.1	0.257	86.5
	1×10^{-5}	457.4	125.1	75.0	0.100	91.1
	5×10^{-5}	482.4	125.0	67.3	0.090	92.0
	1×10^{-4}	483.2	125.3	100.2	0.088	92.2
	5×10^{-4}	491.1	141.0	150.0	0.063	94.4
	1×10^{-3}	500.2	165.4	125.3	0.040	96.0
1 M HCl		507.3	107.1	100.0	1.000	/
	5×10^{-6}	493.0	125.0	150.0	0.398	60.2
	1×10^{-5}	468.0	118.2	100.0	0.316	68.4
	5×10^{-5}	493.0	100.0	93.1	0.159	84.1
	1×10^{-4}	493.4	100.1	100.0	0.123	87.0
	5×10^{-4}	475.0	165.0	93.0	0.100	90.0
	1×10^{-3}	467.0	125.0	92.9	0.081	91.9

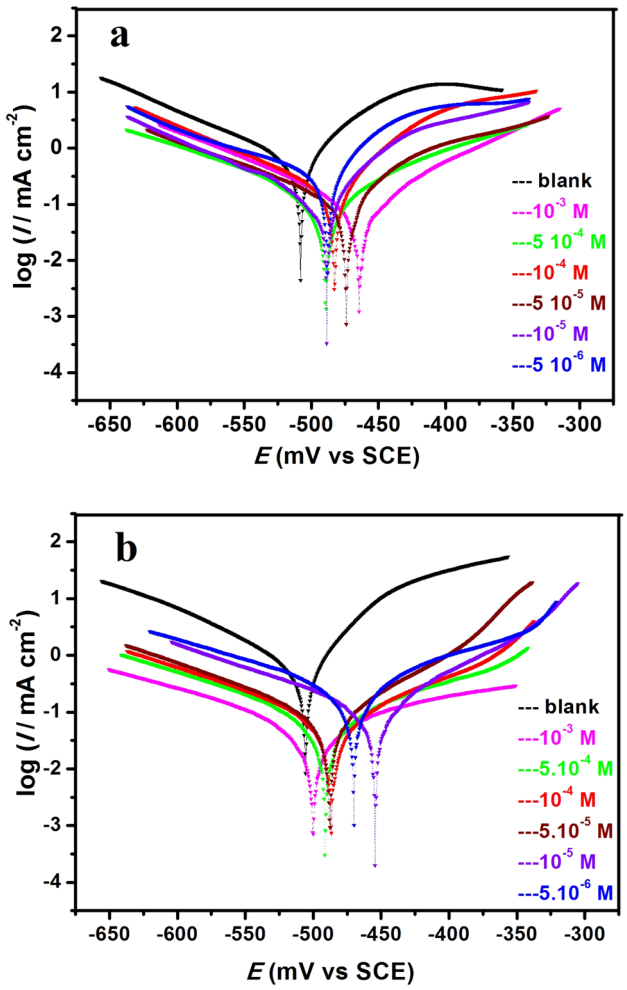

Fig. 2 Tafel curves of carbon steel in **a** 1 M HCl and **b** 0.5 M H_2SO_4 solutions containing different concentrations of ECDYA. Scan rate = 0.5 mV s^{-1}, $T = 293$ K

immersed in 0.5 M H_2SO_4 and 1 M HCl in the absence and presence of different concentrations of ECDYA at 293 K. By extrapolating the Tafel anodic and cathodic linear parts until the straight lines intersect, corrosion current density (i_{corr}), corrosion potential (E_{corr}) as well as polarisation resistance (R) can be determined. A first analysis of these curves (Fig. 2a, b) shows that the anodic and cathodic reactions are affected by the addition of the inhibitor. In fact, in addition to the slight displacement of the free potential towards higher values, the addition of the inhibitor in 1 M HCl solution and 0.5 M H_2SO_4 induces the reduction of the anodic partial current corresponding to the dissolution of the metal and also the decrease of the cathodic current corresponding to the reduction of the proton. The cathodic curves have a linear part (Tafel line) indicating that the hydrogen reduction reaction on the surface of the steel is done according to a pure activation mechanism. This analysis also allows us to see:

-In the cathodic domain, the addition of inhibitor decreases the current densities. The slight modification of the cathodic Tafel slopes (Table 2), in the presence of the inhibitor, in the two media shows that the proton reduction reaction on the surface of the steel is not modified by the addition of the inhibitor and that it is done according to a pure activation mechanism. The inhibitor seems to first adsorb on the surface of the steel before acting by simply blocking its active sites. Such behaviour has also been observed in several studies concerning the same alloy and the same media [44, 45].

-In the same way, in the anode domain, the addition of inhibitor results in a decrease in the densities of the anodic current. In addition, we find for all the concentrations studied, the presence of two linear portions in the case of a strong anodic surge (potential applied to the sample up to − 200 mV/ECS) (is not shown). When a desorption potential Ed, [46], also called potential of unpolarizability by Heusler and Cartledge [47] or by Bartos and Hackerman [48], is exceeded, the inhibitor has practically no longer effect on anode curves; the anodic current density then increases rapidly and the steel dissolves in the region of high overvoltages. This behaviour has been widely documented in the case of steel in hydrochloric acid solutions [49, 50]. The rapid growth of the anodic current, after the potential Ed, is attributed to the desorption of the molecules of the inhibitor adsorbed on the surface of the metal. However, even if the inhibitor resorbs from the metal surface, it inhibits corrosion since the anodic current densities remain lower than those of the white. This clearly indicates that the adsorption and desorption of ECDYA depends on the electrode potential. The phenomenon of inhibition observed is generally described as being due to the formation of an inhibitor layer adsorbed on the surface of the electrode [51]. The variation in ECDYA concentrations in 1 M HCl and 0.5 M H_2SO_4 solutions does not have a significant impact on E_{corr} displacement, as illustrated in Table 2. In literature, an inhibitor can be classified as cathodic or anodic type if the shift of corrosion potential brought about by the inhibitor is higher than 85 mV and as mixed type if the displacement of E_{corr} is lower than 85 mV [52]. In this study, the maximum displacement of E_{corr} values was 51.2 mV versus SCE in H_2SO_4 solution and 38.6 mV versus SCE in HCl solution which indicates that ECDYA acts as mixed type inhibitor in both media. As shown in Table 1, the corrosion rate determined by the weight loss measurement was 1.856 mg cm^{-2} h^{-1} for Hydrochloric acid alone, for example. From Faraday's law, this rate corresponds to a corrosion current density of 1.77 mA cm^{-2} in conformity with the value determined by the Tafel extrapolation method, 1.00 mA cm^{-2} (Table 2). We also note, by examining the inhibitory efficiencies of ECDYA obtained by the EIS (Table 3) and those obtained

Table 3 The EIS parameters of carbon steel in 0.5 M H_2SO_4 and 1 M HCl solutions in the presence and absence of various concentrations of ECDYA at 293 K

Acid solutions	C_{inh} (M)	R_s (Ω cm^2)	R_{ct} (Ω cm^2)	Q 10^{-6} (S^n Ω^{-1} cm^{-2})	n	C_{dl} (μF cm^{-2})	IE_{Rct} (%)
0.5 M H_2SO_4	0	1.394	12.32	3112.8	0.932	2453.7	/
	5×10^{-6}	1.877	43.86	1372.3	0.884	949.1	71.91
	1×10^{-5}	1.799	66.47	1084.1	0.880	757.4	81.46
	5×10^{-5}	1.279	78.20	977.1	0.828	572.7	84.24
	1×10^{-4}	1.843	120.36	952.5	0.756	473.4	89.76
	5×10^{-4}	2.162	196.17	657.4	0.783	372.7	93.72
	1×10^{-5}	2.854	247.45	696.9	0.703	331.7	95.02
1 M HCl	0	1.334	33.42	1125.5	0.774	431.9	/
	5×10^{-6}	1.540	107.46	409.8	0.783	172.5	68.90
	1×10^{-5}	1.663	151.06	274.8	0.797	122.2	77.88
	5×10^{-5}	1.934	190.06	258.5	0.805	124.6	82.42
	1×10^{-4}	1.993	201.10	241.8	0.813	120.6	83.38
	5×10^{-4}	1.320	230.03	166.7	0.824	83.1	85.47
	1×10^{-3}	1.302	251.14	164.8	0.822	82.7	86.69

by the polarisation curves (Table 2), that these efficiencies have been confirmed.

3.3 EIS Measurements

The study, by EIS at 293 K, of the corrosion of carbon steel in 1 M HCl and 0.5 M H_2SO_4 solutions in the absence and presence of various concentrations of ECDYA was also carried out. The following equation illustrates the formula used in the calculation of the inhibitor efficiency:

$$IE_{EIS}\% = \left(\frac{R'_{ct} - R_{ct}}{R'_{ct}}\right) \times 100 \quad (16)$$

where R_{ct} and R'_{ct} represent the resistance of charge transfer in the absence and presence of inhibitor, respectively. The impedance spectra for Nyquist plots (Fig. 3a, b) were analysed by fitting data to equivalent circuit model (Fig. 4), which was used to describe carbon steel/solution interface. A basic electrical equal circuit (EEC) has been proposed to show the test information. In this circuit R_s is the resistance of solution, R_{ct} is the resistance of charge transfer and CPE (Q) represents the constant phase element that replaces the capacitance of the electric double layer (C_{dl}) [53–55]. Excellent fits with this model were obtained for all experimental data. The interfacial capacitance C_{dl} and the polarisation resistance were calculated from the CPE parameter according to the following equation [56]:

$$C_{dl} = R_{ct}^{\frac{1-n}{n}} \times Q^{\frac{1}{n}} \quad (17)$$

where n is the deviation parameter of the CPE:$0 \le n \le 1$. For $n=1$, Eq. (17) agrees with the impedance of an ideal capacitor, where Q is identified as the capacity. The electrochemical

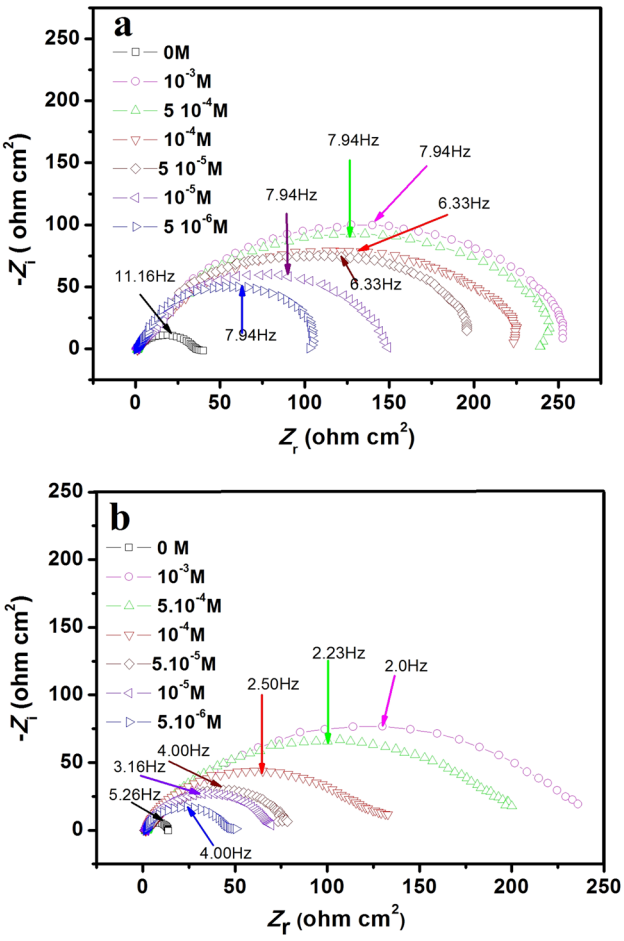

Fig. 3 Nyquist diagrams of carbon steel obtained at 293 K in solutions of **a** 1 M HCl alone and **b** 0.5 M H_2SO_4 alone and in these media containing different concentrations of ECDYA

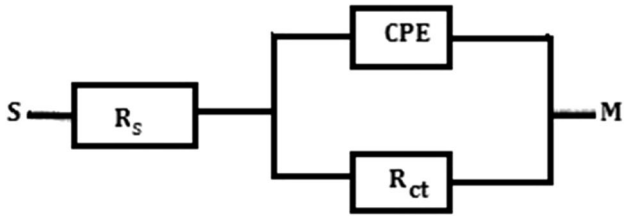

Fig. 4 The model used as a circuit equivalent to the metal-solution interface for determining EIS data

parameters including R_{ct}, Q, and n, obtained from the fit, are listed in Table 3. The calculated double-layer capacitance values are also given in Table 3. The results obtained in the form of Nyquist plots (Fig. 3a, b) have been exploited. These diagrams obtained consist of a single capacitive loop which is not a perfect half circle; this is attributed to the dispersion of the frequency of the interfacial impedance due to the heterogeneity of the surface of the electrode [55]. This heterogeneity may result from roughness, impurities and dislocations, adsorption of the inhibitor and formation of the porous layer [57]. This type of diagram is generally interpreted as a mechanism of charge transfer over a heterogeneous and irregular surface [58, 59]. In addition, these diagrams have a similar shape for all tested concentrations, indicating that there is no change in the mechanism of corrosion [60], and the diameter of the capacitive semicircles increases with the increasing the concentration of the inhibitor. The EIS results confirm that ECDYA inhibits the corrosion of carbon steel in 1 M HCl and 0.5 M H_2SO_4 at 293 K for all investigated concentrations, with a continuous increase of the inhibition efficiency (*IE*) with the increase in concentration. From Table 4, it is clear that the charge transfer resistance (R_{ct}, Ω cm^2) increases, the double-layer capacitance (C_{dl}, μF cm^{-2}) decreases and the inhibitor efficiency (*IE*%) increases as the inhibitor concentration increases.

Some ketene dithioacetal derivatives belonging to the same family of ECDYA have been studied by Fiala et al. [24, 61] for copper corrosion in 3 M HNO_3 at different concentrations and at 298 K using chemical and electrochemical measurements. The results show that these products inhibit the corrosion of copper in this medium. The corrosion rate depends on the concentration of the inhibitor. Increasing the concentration of each derivative increases the effectiveness of the inhibition up to a maximum value (100% at 10^{-3} M for compound 1, 96% at 10^{-3} M for compound 2 and 90% at 10^{-3} M for compound 3). The inhibitory efficiency of ECDYA reached 81% in HCl 1 M and 98% in H_2SO_4 0.5 M at the same concentration (10^{-3} M) for corrosion of carbon steel. This suggests that derivatives belonging to this family of compounds can be used as inhibitors of corrosion of metals and their alloys in acidic environments.

3.4 Adsorption Isotherm and Thermodynamic Consideration

The inhibitory action of inhibitors in acidic media is generally due to the adsorption of their molecules on the metal surface. Therefore, and for a highlight on the mechanism of this process, we have chosen in this work to study the adsorption behaviour of ECDYA on carbon steel, in hydrochloric and sulphuric acid media, in a concentration range from 5×10^{-6} to 10^{-3} M at 293 K. Several adsorption isotherms were tested. The fraction of the surface covered, θ, by the adsorbed inhibitor is expressed as a function of the inhibitory efficiency, *EI*%, by the following relation:

$$\theta = EI\%/100 \tag{18}$$

where *EI*% is evaluated from the gravimetric method. Adsorption of ECDYA on the surface of the steel in HCl and H_2SO_4 solutions have been found to follow the Langmuir adsorption isotherm, as can be seen clearly (Fig. 5) that the curves representing C/θ versus C (concentration of the inhibitor) in 1 M HCl and 0.5 M H_2SO_4 are straight lines with slopes close to 1 and values correlation coefficients (R^2) ranging from 0.9993 to 0.9997 in the first corrosive medium and from 0.9987 to 0.9998 in the second. However, by analysing the equations of the experimental lines obtained we notice that the slopes are slightly greater than unity. This

Table 4 Thermodynamic parameters of adsorption of ECDYA on the surface of steel in acidic media at different temperatures

Acid solutions	T (K)	K_{ads} (M^{-1})	ΔG_{ads} (kJ mol^{-1})	ΔH_{ads} (kJ mol^{-1})	ΔS_{ads} (J mol^{-1} K^{-1})
0.5 M H_2SO_4	293	1.377×10^5	−38.6	−14.1	83.5
	303	1.028×10^5	−39.2		
	313	1.090×10^5	−40.6		
	323	7.429×10^4	−40.9		
1 M HCl	293	1.115×10^5	−38.1	−25.2	43.7
	303	7.580×10^4	−38.4		
	313	4.724×10^4	−38.5		
	323	4.560×10^4	−39.6		

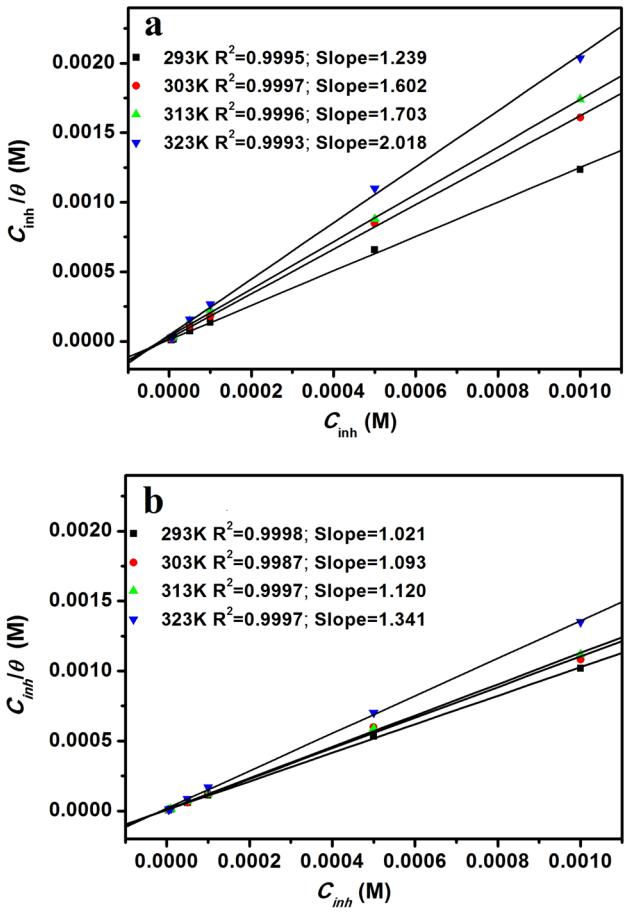

Fig. 5 Langmuir isotherm of the system: carbon steel and The ECDYA inhibitor in **a** 1 M HCl and **b** 0.5 M H_2SO_4, at different temperatures

result shows that ECDYA occupies several active sites. Thus the values of the thermodynamic parameters were calculated from the modified Langmuir model given by the following equation [62]:

$$C/\theta = n/K_{ads} + nC \tag{19}$$

where C is the inhibitor concentration (mol L^{-1}), K_{ads} is the adsorption equilibrium constant (L mol^{-1}) and θ is the fraction of surface covered with inhibitor. The values of the equilibrium constants of the adsorption process are related to the standard free energy of adsorption by the relation [63]:

$$K_{ads} = \left(\frac{1}{55.5}\right)\exp\left(\frac{-\Delta G^{\circ}_{ads}}{RT}\right) \tag{20}$$

where R is the universal constant of gas and T is the temperature in Kelvin. The value of 55.5 represents the concentration of water in solution (mol L^{-1}). The influence of the temperature on the adsorption equilibrium constant, K_{ads}, can be expressed according to the following relation (the integrated form of the Van 't Hoff equation):

$$\ln K_{ads} = \left(\ln\frac{1}{55.5} + \frac{\Delta S_{ads}}{R}\right) - \left(\frac{\Delta H_{ads}}{RT}\right) \tag{21}$$

where R is the perfect gas constant, T is the absolute temperature and ΔH_{ads} is the adsorption enthalpy and ΔS_{ads} is the adsorption entropy. The ΔH_{ads} and the ΔS_{ads} values were deduced from the plot of ln K_{ads} as a function of 1/T (not shown). This plot gave straight lines with a correlation coefficient close to unity. The intersection of each line is equal to the constant (ln 1/55.5 + $\Delta S_{ads}/R$), allows the determination of ΔS_{ads} and, the slope is equal to $-\Delta H_{ads}/R$. The estimations of these parameters are given in Table 4. The spontaneity of the adsorption process and stability of the adsorbed layer on the surface of the carbon steel are confirmed by the appearance of the negative sign in the values of ΔG_{ads}. These values for all the studied systems lie between −38.1 and −40.9 kJ mol^{-1} in both acidic medium, indicating that the adsorption of the evaluated inhibitor on the carbon steel surface may include complex connections (both physical and chemical adsorption). On the other hand, the decrease observed for K_{ads} and *IE* with the temperature rise suggests that ECDYA molecules are physically adsorbed on the metal surface, thus favouring the desorption process. The latter also appeared in the values of ΔH_{ads} indicating the exothermic nature of the adsorption process of the inhibitory molecules [3, 64–66]. An exothermic adsorption process can be chemical, physical or a mixture of both [67], whereas the endothermic process is attributed to chemisorption [68]. In an exothermic process, physisorption is distinguished from chemisorption by the absolute value of the adsorption enthalpy: when the latter is less than 40 kJ mol^{-1}, a physisorption mechanism is operating, the enthalpy of chemisorption being closer to 100 kJ mol^{-1} [69]. In the present study, the enthalpy absolute values indicate that physisorption is the process that took place. Positive values of the entropy were observed in both media relating the substitutional process. This means that an increase in disorder took place probably because when one inhibitor molecule adsorbs onto the metal surface many more water molecules are desorbed. Together with ΔH_{ads}, this constitutes the driving force for the adsorption of inhibitor onto steel [70, 71].

3.5 Activation parameters of the inhibition process

The temperature can modify the interaction between the mild steel electrode and the acidic medium in absence and presence of the inhibitor [3]. Some experiments were performed in order to evaluate this interaction, to calculate the activation parameters of the corrosion process of carbon steel in both acidic solutions and to test the anticorrosion

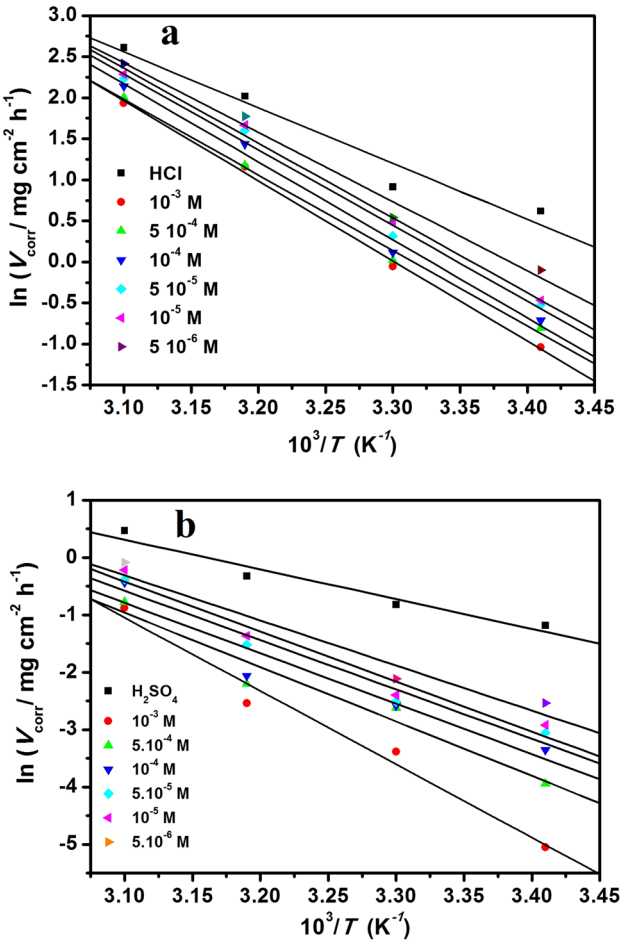

Fig. 6 ln V_{corr} versus $1/T$ curve of dissolution of carbon steel in **a** 1.0 M HCl and **b** 0.5 M H_2SO_4 solutions with and with various concentrations of ECDYA

property of the inhibitor. Thus, weight loss measurements were made in the range of temperature 293–323 K in the absence and presence of different concentrations of ECDYA, after a 5 h immersion into 1 M HCl and 0.5 M H_2SO_4 solutions. Corrosion reactions can be regarded as Arrhenius-type processes; therefore, the Arrhenius equation was used in the calculation of activation parameters:

$$\ln V_{corr} = \ln A + \left(\frac{-E_a}{RT}\right) \tag{22}$$

where V_{corr} is the corrosion rate, E_a is the apparent activation energy, R is the universal gas constant, T is the absolute temperature and A is the pre-exponential factor.

Figure 6 shows the Arrhenius plots of ln V_{corr} versus $1/T$ for corrosion of carbon steel in 1 M HCl and 0.5 M H_2SO_4 solutions without and with the addition of different concentrations of ECDYA. A plot of ln V_{corr} versus $1/T$ obtained from weight loss measurements gave a straight line with a regression coefficient close to unity. The values of apparent activation energy (E_a) obtained from the slope $-E_a/R$ of the lines and the pre-exponential factor (A) obtained from the intercept ln A are displayed in Table 5. The enthalpy of activation (ΔH_a) and the entropy of activation (ΔS_a) were calculated using the transition equation (Eq. (23)):

$$\ln (V_{corr}/T) = \{\ln(R/Nh) + (\Delta S_a/RT)\} - (\Delta H_a/RT) \tag{23}$$

where N is Avogadro's number and h is Plank's constant.

Figure 7 shows that the plots of ln (V_{corr}/T) with respect to $1/T$, also gave straight lines, for carbon steel dissolution in 1 M HCl and in 0.5 M H_2SO_4 in the absence and presence of different concentrations of ECDYA. The slope of each line equals its respective $-\Delta H_a/R$ term while the intercept equals ln $(R/Nh)+\Delta S_a/R$. The values of ΔS_a and ΔH_a were

Table 5 Thermodynamic activation parameters of carbon steel dissolution in 1 M HCl and 0.5 M H_2SO_4 solutions with and without various concentrations of ECDYA

Acid solutions	*Conc.* of ECDYA (M)	E_a (kJ mol^{-1})	ΔH_a (kJ mol^{-1})	ΔS_a (J mol^{-1} K^{-1})
0.5 M H_2SO_4	0	43.0	40.1	−118.8
	5×10^{-6}	65.2	62.0	−56.0
	1×10^{-5}	72.2	69.7	−33.0
	5×10^{-5}	71.3	68.0	−39.5
	1×10^{-4}	73.1	70.64	−33.0
	5×10^{-4}	79.3	76.7	−15.5
	1×10^{-3}	107.8	104.8	70.7
1 M HCl	0	56.1	53.0	−60.1
	5×10^{-6}	69.8	66.4	−19.6
	1×10^{-5}	75.4	71.9	−3.2
	5×10^{-5}	76.3	72.8	−1.00
	1×10^{-4}	78.6	75.2	5.4
	5×10^{-4}	76.2	72.8	−3.5
	1×10^{-3}	80.8	77.3	10.2

subsequently calculated from these terms and presented in Table 5. The obtained results of this study show that the E_a values ranged from 65.16 to 107.75 kJ mol^{-1} for the inhibited H_2SO_4 solution and from 69.78 to 80.76 kJ mol^{-1} for the inhibited HCl solution. It's clear that the apparent activation energy (E_a) increased with increasing concentration of ECDYA and was higher than that in the absence of inhibitor (Table 5). This indicates that the corrosion reaction of CS is inhibited by ECDYA and supports the phenomenon of physical adsorption [12, 72, 73]. In this case, the continuous increase in activation energy with the concentration of the inhibitor makes the corrosion process more difficult (higher energy barrier) which can be attributed to an increase in thickness of the double layer [74], giving strong anti-corrosive properties to ECDYA and enhancing the electrostatic characteristics of adsorption of the inhibitor on the CS surface (physisorption) [75]. The endothermic nature of the carbon steel dissolution process is revealed by the positive sign of the enthalpy values of activation, thus expressing its difficult course. The negative sign of the activation entropy values either in the absence or in the presence of the inhibitor may be explained by the fact that during the formation of the activated complex and in the determining step of the reaction the reaction is associative rather than dissociative, meaning that a decrease in disorder occurs starting from the reagents to the activated complex [76, 77].

At higher concentration (10^{-3} M), a positive value of the entropy of activation was observed in both media. This indicates that the system passes from a more ordered state to a more random arrangement [78].

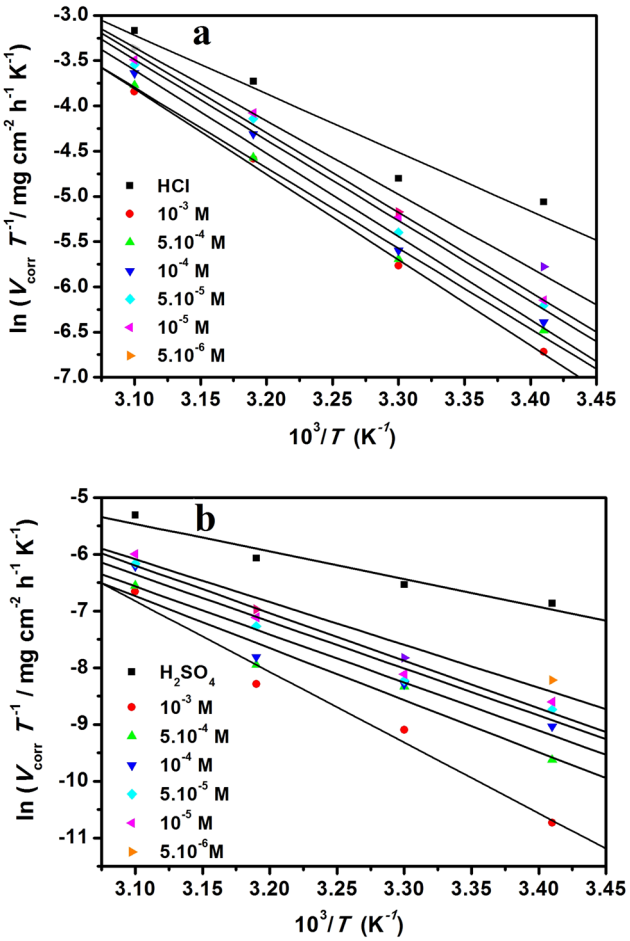

Fig. 7 ln V_{corr}/T versus $1/T$ for carbon steel dissolution in **a** 1 M HCl and **b** 0.5 M H_2SO_4 without and with different concentrations of ECDYA

3.6 Surface analysis

The SEM images were recorded (Fig. 8a–e) in order to establish the interaction of inhibitor molecules with the metal surface. Figure 8a shows the polished lines on the surface of steel before its exposure to the testing environments. Figures 8b and c show the SEM images of steel after immersion in 1 M HCl and 0.5 M H_2SO_4 solutions, respectively. These reveal severe damage on the surface, in both acidic media, due to metal dissolution. Indeed, the metal surface immersed in both blank acid solutions appears rough, with plenty of pits and cavities at certain regions. In contrast, Figures 8d and e show a smooth steel surface after adding 1 mM of ECDYA, indicating a protected surface. These images suggest that the protection comes from the formation of ECDYA layer on the CS surface that prevents the attack of acids.

3.7 Properties of Inhibitor and Inhibitive Mechanism

Weight loss results indicate that ECDYA is effectively an inhibitor of carbon steel corrosion in acidic media. The polarisation curves show that metal dissolution and cathodic reduction reactions were inhibited by adding ECDYA to the acidic solution. This inhibition is more pronounced by increasing the concentration of the latter. The curves of the cathodic branch make it possible to obtain parallel Tafel lines with slopes (β_c) of very close values indicating that the addition of the inhibitor to the aggressive medium does not modify the mechanism of the proton reduction and that this reaction is under pure activation control. This suggests that the inhibitor is first adsorbed on the metal surface and then acts by blocking the active sites of the carbon surface. In this way, the area exposed to H^+ ions is decreased, but the mechanism of the reaction remains intact [79]. This indicates that the mode of action of this inhibitor is due to its adsorption on the surface of the metal. The analysis of impedance spectra obtained by electrochemical impedance spectroscopy also shows that the corrosion rate of steel is decreased in the presence of ECDYA. And because this decrease in the rate of corrosion is related to the decrease

of C_{dl} values and it is well established that the decrease of the values of the capacity of the double layer, C_{dl} can occur only if there is a decrease the local dielectric constant and/or an increase in the thickness of the double layer [80], it can once again be concluded that the molecules of this inhibitor adsorb on the metal surface thus preventing the strong attack of the aggressive agent. The study of surface morphology of carbon steel samples emerged in 1 M HCl and 0.5 M H_2SO_4 solutions in the absence and in the presence of 1 mM ECDYA revealed that severe surface damage suffered in the absence of ECDYA was attenuated in his presence. This suggests that the molecules of this inhibitor serve as a shield by adsorbing at the steel/acid interface thus weakening the attacks of the aggressive agent of the medium. The calculation of the ΔG_{ads} values (Table 4) indicates that the value of ΔG_{ads} is between the values of the physical adsorption and those of the chemical adsorption thus showing that the adsorption of the ECDYA on the surface of the steel is serving two types of interaction [81]. It can, therefore, be considered that the inhibitory action of this compound is carried out by the following two routes:

(a) Physisorption

This process occurs after the protonation of the inhibitor molecules in each of the two media studied according to Eq. (24).

$$\mathrm{In} + \mathrm{H}^{+} \rightarrow \mathrm{InH}^{+}(\mathrm{In}: \text{ inhibitor molecule}) \tag{24}$$

Likhanova et al. [82], summarised the reactions of the anodic dissolution of metals (M) in acidic aqueous solutions (e.g. H_2SO_4) as follows:

$$\mathrm{M} + \mathrm{nH_2O} \leftrightarrow \mathrm{M(H_2O)n_{ads}} \tag{25}$$

$$\mathrm{M\,(H_2O)}n_{\mathrm{ads}} + \mathrm{SO_4^{2-}} \leftrightarrow \mathrm{M\,[(H_2O)}_n\mathrm{SO_4^{2-}]_{ads}} \tag{26}$$

$$\mathrm{M\,[(H_2O)}_n\mathrm{SO_4^{2-}]_{ads}} \rightarrow \mathrm{M\,(H_2O)}_n\mathrm{SO_4]_{ads}} + 2e^{-} \tag{27}$$

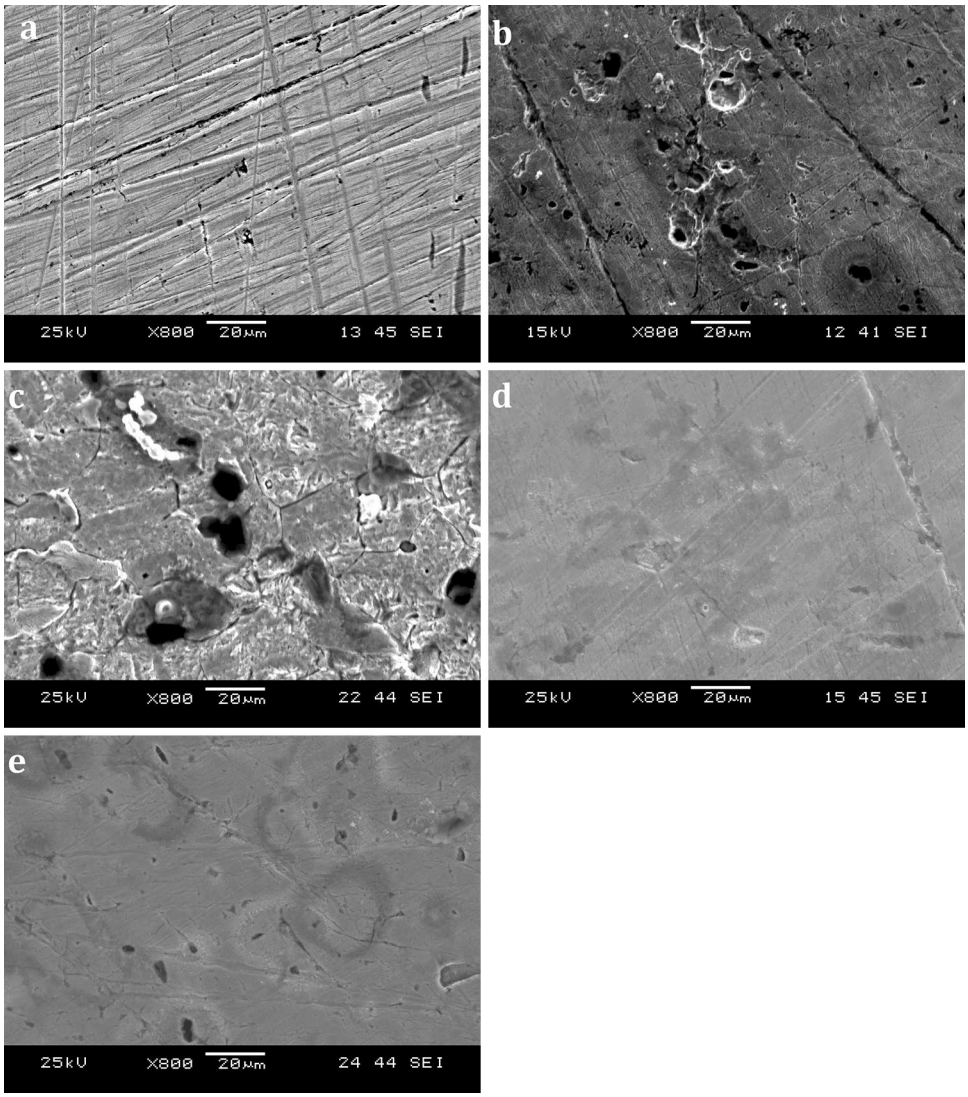

Fig. 8 Images obtained by SEM of the steel surfaces **a** before corrosion and after immersion for 3 h at 293 K in **b** 1 M HCl, **c** 0.5 M H_2SO_4, **d** 1 M HCl + 1 mM ECDYA) and **e** 0.5 M H_2SO_4 + 1 mM ECDYA

$$[M(H_2O)_nSO_4]_{ads} \rightarrow M^{2+} + OH^- + SO_4^{2-} + H^+ \quad (28)$$

It can be thought that the charged molecules of the inhibitor which are present in these solutions prevent the progress of step (27) and consequently step (28) by forming a monomolecular layer as a complex on the carbon steel surface (Eq. (29)).

$$M[(H_2O)_nSO_4^{2-}]_{ads} + InH^+ \rightarrow ([M(H_2O)_nSO_4]InH)^-_{ads} \quad (29)$$

In addition to the formation of this monomolecular layer, according to this same reference, the formation of inhibitor multilayer of $InH^+ SO_4^{2-} InH^+$ (Eq. (30)) is not sidelined. The multilayer is stabilised by Van der Waals cohesion forces between the charged form of the inhibitor molecule and the counter ion of the protic acidic solution [83], which allows the formation of a more closely film on the metal/solution interface.

$$\begin{aligned}&([M(H_2O)_nSO_4]InH)^-_{ads} + InH^+ + SO_4^{2-}\\ &\rightarrow ([M(H_2O)_nSO_4]_{ads}InH)^-InH^+SO_4^{2-}/InH^+))_{ads}\end{aligned} \quad (30)$$

For the inhibition of the cathodic evolution of hydrogen, it can be seen as follows: The presence of the molecule of the inhibitor in the corrosive solution delays the rate of the reaction of Volmer ($M + H^+ + e^- \leftrightarrow MH_{ads}$) representing the first step in the Volmer–Tafel mechanism describing the evolution of hydrogen or decreases the rate of the Heyrovsky reaction ($MH_{ads} + H^+ + e^- \leftrightarrow H_2 + M$) forming the second step of the Volmer–Heyrovsky mechanism leading to the formation of hydrogen gas, and this, thanks to the competition in the consumption of the electrons of this molecule charged with the hydrogen ion according to the following equation:

$$M + InH^+ + e^- \leftrightarrow M(InH)_{ads} \quad (31)$$

(b) Chemisorption

The molecules of this inhibitor (ECDYA) in their neutral (non-protonated) form transfer their free electrons from the heteroatoms they possess (O, N and S) and the π-electrons from the multiple bonds to the d-orbitals of iron atoms at the surface of the metal leading to the formation of coordination bonds between the metal and these molecules in the same way as several organic inhibitors [84–87].

3.8 Quantum Chemical Calculations

The computed total energies at the DFT CAM-B3LYP/def2-TZVPP level for optimised structures of the two possible isomers (Fig. 9), confirms that compound 2 is more stable than the isomer 1. We then focus our analysis on the local reactivity of the isomers 2 in order to predict the reactive sites of this compound. The molecular structure of isomers 2 and the atom-numbering structure are shown in Fig. 1. The optimised molecular structures and the frontier molecule orbital density distribution of the title molecule are given in Fig. 10, and the calculated quantum chemical parameters are listed in Table 6. The distribution of the electron density HOMO and LUMO of the molecule is shown in Fig. 10. It is observed that the distribution of the density HOMO (blue regions) is localised on the heteroatoms (N, O and S) indicating the preferred sites for a electrophilic attack of metal cations. On the other hand, the distribution of the electronic density LUMO (brown regions) is localised on the centres –S–, –C– S–, –C=O and –C≡N indicating the sites able to accept electrons, which can also show that the molecule can certainly accept electrons. HOMO energy (E_{HOMO}) indicates the tendency of a molecule to give electrons to a suitable low energy acceptor molecule or an empty electron orbital, whereas the LUMO energy (E_{LUMO}) characterises the sensitivity of the molecule to a nucleophilic attack [88]. In-depth analysis of these orbitals shows that the HOMO and LUMO are localised mainly on the S1, S2, C2, C4 and N1 atoms, with proportions of the 18% (S1), 32% (S2), 30% (C2) and 10% (N1) in HOMO, and 12.7% (S1), 10% (S2), 14% (C2) and 36% (C4) in LUMO orbitals. These results revealed the reactive sites of the inhibitor molecule susceptible to electrophilic and nucleophilic attacks with the steel surface. The dipole moment (μ) value of ECDYA (7.7564 D) was much higher than that of H_2O (1.8546 D), demonstrating that the investigated ECDYA inhibitor was tending to adsorb on the

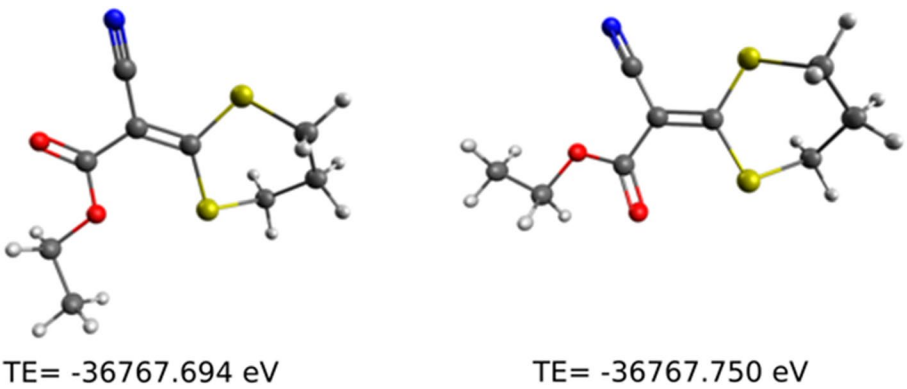

Fig. 9 DFT- optimised structures of the two possible isomers

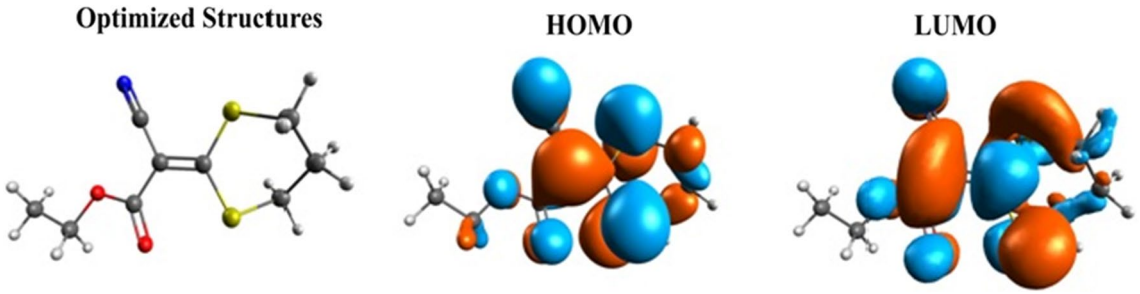

Fig. 10 Optimised structures, HOMO and LUMO of ECDYA at CAM-B3LYP/311 ++G(d,p)

Table 6 Calculated quantum chemical parameters of the title compound at CAM-B3LYP/311 ++G(d,p) level

Inhibitor	$E_{HOMO\ (eV)}$	$E_{LUMO\ (eV)}$	ΔE (eV)	η	σ	χ	μ (Debye)	ΔN
ECDYA	−7.9622	−0.9878	6.9744	3.4872	0.2868	4.4750	7.7564	−0.0595

metallic surface as a replacement for H_2O molecular which leads to good protection.

The natural population analysis (NPA), ChelpG [89] and Mulliken charge analysis (collected in Table 7) have been calculated in order to provide a quantitative description of the electron density redistribution. In view of the above results, the O1 atom has more negative charge followed by O2, C7 and C9, therefore suggests that, a greater electron donor character of the O1 atom than the other sites. It should also be noted, that this inhibitor molecule has a greater tendency to adsorb on the steel surface as it represents several highly negative charged centres (O1, O2, C7 and C9). In addition, analysis of the local reactivity and regioselectivity of our inhibitor structure (Table 7), investigated by Fukui indices under Mulliken populations show that the S2 atom is associated with the maximum values of f+ and f−, and therefore reveals that this atom is likely to be engaged in both nucleophilic and electrophilic attack. However, the positive sign of Δf indicating that the S2 atom is more susceptible to nucleophilic than electrophilic attack. Figure 11 schematically illustrates the agreement of assumptions and conclusions drawn from the experimental results with those contemplated by quantum chemical calculations.

Table 7 Calculated atomic charges on the selected atom of the title compound at CAM-B3LYP/311 ++G(d,p) level

Atoms	Mulliken	NPA	ChelpG
S2	0.037	0.406	−0.072
S1	−0.009	0.335	−0.102
O1	−0.402	−0.640	−0.660
O2	−0.268	−0.485	−0.404
N1	−0.064	−0.413	−0.613
C1	0.362	0.787	0.848
C2	0.004	−0.390	−0.433
C3	−0.229	0.334	0.474
C4	0.002	−0.231	0.230
C5	−0.185	−0.520	−0.011
C6	−0.142	−0.422	−0.094
C7	−0.203	−0.539	0.007
C8	0.005	−0.076	0.323
C9	−0.285	−0.623	−0.437

4 Conclusion

The main conclusions drawn from this examination are:

Ethyl 2-cyano-2-(1,3-dithian-2-ylidene) acetate (ECDYA) effectively inhibits carbon steel corrosion in 0.5 M H_2SO_4 and 1 M HCl solutions and the inhibition efficiency increases with inhibitor concentration at all temperatures studied. The polarisation curves show that this inhibitor is of the mixed type. The Langmuir adsorption isotherm is best suited for expressing the adsorption process of the inhibitor at the surface of the carbon steel, and the negative value of the Gibbs free energy of adsorption (ΔG_{ads}) is indicative of a strong interaction between the inhibitor molecules and the surface of carbon steel. The protection proprieties of ECDYA for carbon steel corrosion are better in 0.5 M H_2SO_4 than in 1 M HCl. The increasing value of CPE exponent (n) with increasing inhibitor concentration indicated that the surface roughness decreased with increasing inhibitor concentration. The SEM study agrees with this conclusion. The measurements of weight loss, polarisation and electrochemical impedance

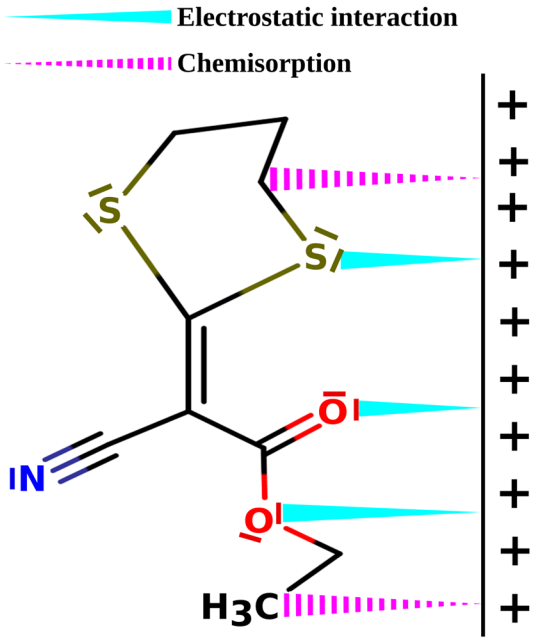

Fig. 11 Schematic representation of the adsorption component of ECDYA on the carbon steel surface in corrosive media (HCl or H_2SO_4 solution)

spectroscopy are in good agreement. The DFT study also confirms the inhibitory action of ECDYA by adsorption.

Compliance with Ethical Standards

Conflict of interest On behalf of all authors, the corresponding author states that there is no conflict of interest.

References

1. Kalla A, Benahmed M, Djeddi N, Akkal S (2016) Corrosion inhibition of carbon steel in 1 M H_2SO_4 solution by *Thapsia villosa* extracts. Int J Ind Chem 7:419–429
2. Pradeep Kumar CB, Mohana KN (2014) Corrosion inhibition efficiency and adsorption characteristics of some Schiff bases at mild steel/hydrochloric acid interface. J Taiwan Inst Chem Eng 45:1031–1042
3. Daoud D, Douadi T, Issaadi S, Chafaa S (2014) Adsorption and corrosion inhibition of new synthesized thiophene schiff base on mild steel X52 in HCl and H_2SO_4 solutions. Corros Sci 79:50–58
4. Ali SA, Al Muallem HA, Rahman SU, Saeed MT (2008) Bis-isoxazolidines: a new class of corrosion inhibitors of mild steel in acidic media. Corros Sci 50:3070–3077
5. El Achouri M, Kertit S, Gouttaya HM, Nciri B, Bensouda Y, Perz L, Infante MR, El Kacemi K (2001) Corrosion inhibition of iron in 1 M HCl by some Gemini surfactants in the series of Alkanediyl-α, ω-bis-(dimethyl tetradecyl ammonium bromide). Prog Org Coat 43:267–273
6. Memari B, El Attari H, Traisnel M, Bentiss F, Lagrenee M (1998) Inhibiting effects of 3,5-bis(n-pyridyl)-4-amino-1,2,4-triazoles on the corrosion for mild steel in 1 M HCl medium. Corros Sci 40:391–399
7. Abboud Y, Tanane O, El Bouari A, Salghi R, Hammouti B, Chetouani A, Jodeh S (2016) Corrosion inhibition of carbon steel in hydrochloric acid solution using pomegranate leave extracts. Corros Sci Techn 51:557–565
8. Gopiraman M, Selvakumaran N, Kesavan D, Karvembu R (2012) Adsorption and corrosion inhibition behavior of N- (phenylcarbamothioyl) benzamide on mild steel in acidic medium. Prog Org Coat 73:104–111
9. Yadav DK, Quraishi MA, Maiti B (2012) Inhibition effect of some benzylidenes on mild steel in 1 M HCl: an experimental and theoretical correlation. Corros Sci 55:254–266
10. Yuce AO, Solmaz R, Karda G (2012) Investigation of inhibition effect of rhodamine-N-acetic acid on mild steel corrosion in HCl solution. Mater Chem Phys 131:615–620
11. Keles H (2011) Electrochemical and thermodynamic studies to evaluate inhibition effect of 2-[(4-phenoxy-phenylimino) methyl]-phenol in1 M HCl on mild steel. Mater Chem Phys 130:1317–1324
12. Kosari A, Momeni M, Parvizi R, Zakeri M, Moayed MH, Dvoodi A, Eshghi H (2011) Theoritical and electrochemical assessment of inhibitive behavior of some thiophenol derivatives on mild steel in HCl. Corros Sci 53:3058–3067
13. Solmaz R (2014) Investigation of corrosion inhibition mechanism and stability of Vitamin B1on mild steel in 0.5 M HCl solution. Corros Sci 81:75–84
14. Doner A, Sahin EA, Kardas G, Serindag O (2013) Investigation of corrosion inhibition effect of 3-[(2-hydroxy-benzylidene)amino]-2-thioxo-thiazolidin-4-one on corrosion of mild steel in the acidic medium. Corros Sci 66:278–284
15. Doner A, Yüce AO, Kardas G (2013) Inhibition effect of rhodamine-N-acetic acid on copper corrosion in acidic media. Ind Eng Chem Res 52:9709–9718
16. Solmaz R, Sahin EA, Doner A, Kardas G (2011) The investigation of synergistic inhibition effect of rhodamine and iodide ion on the corrosion of copper in sulphuric acid solution. Corros Sci 53:3231–3240
17. Solmaz R (2010) Investigation of the inhibition effect of 5-((E)-4-phenylbuta-1,3-dienyllidene-amino)-1,3,4-thiadiazole-2-thiol Schiff base on mild steel corrosion in hydrochloric acid. Corros Sci 52:3321–3330
18. Emregül KC, Hayvali M (2004) Studies on the effect of vanillin and protocatechualdehyde on the corrosion of steel in hydrochloric acid. Mater Chem Phys 83:209–216
19. Goulart CM, Esteves-Souza A, Martinez-Huitle CA, Rodrigues CJF, Maciel MAM, Echevarria A (2013) Experimental and theoretical evaluation of semi carbazones and thiosemicarbazones as organic corrosion inhibitors. Corros Sci 67:281–291
20. Aljourani J, Golozar MA, Raeissi K (2010) The inhibition of carbon steel corrosion in hydrochloric and sulfuric acid media using some benzimidazole derivatives. Mater Chem Phys 121:320–325
21. Hasanov R, Bilge S, Bilgiç S, Gece G, Kiliç Z (2010) Experimental and theoretical calculations on corrosion inhibition of steel in 1 M H_2SO_4 by crown type polyethers. Corros Sci 52:984–990
22. Xu F, Duan J, Zhang S, Hou B (2008) The inhibition of mild steel corrosion in 1 M hydrochloric acid solutions by triazole derivative. Mater Lett 62:4072–4074
23. Khan G, Basirun WJ, Kazi SN, Ahmed P, Magaji L, Ahmed SM, Khan GM, Abdur Rehman M (2017) Electrochemical investigation on the corrosion inhibition of mild steel by Quinazoline Schiff base compounds in hydrochloric acid solution. J Colloid Interface Sci 502:134–145
24. Fiala A, Chibani A, Darchen A, Boulkamh A, Djebbar K (2007) Investigation of the inhibition of copper corrosion in nitric

acid solutions by ketene dithioacetal derivatives. Appl Surf Sci 253:9347–9356
25. Yanai T, Tew DP, Handy NC (2004) A new hybrid exchange-correlation functional using the Coulomb-attenuating method (CAM-B3LYP). Chem Phys Lett 393(1–3):51–57
26. Boukhedena W, Fiala A, Brahim Ladouani H, Lemallem SE, Hamdounib N, Boudjada A (2018) Crystal structure of ethyl 2-cyano-2-(1,3-dithian-2-ylidene)acetate. Acta Cryst E 74:65–68
27. Neese F (2018) Software update: the ORCA program system, version 4.0. Wiley Interdiscip Rev 8:1327
28. Neese F (2012) The ORCA program system. Wiley Interdiscip Rev Comput Mol Sci 2:73–78
29. Weigend F, Ahlrichs R (2005) Balanced basis sets of split valence, triple zeta valence and quadruple zeta valence quality for H to Rn: design and assessment of accuracy. Phys Chem Chem Phys 7:3297–3305
30. Hanwell MD, Curtis DE, Lonie DC, Vandermeersch T, Zurek E, Hutchison GR (2012) Avogadro: an advanced semantic chemical editor, visualization, and analysis plat- form. J Cheminform 4(1):17
31. Koopmans T (1934) Über die Zuordnung von Wellenfunktionen und Eigenwerten zu den Einzelnen Elektronen Eines Atoms. Physica 1:104–113
32. Allal H, Belhocine Y, Zouaoui E (2018) Computational study of some thiophene derivatives as aluminium corrosion inhibitors. J Mol Liq 265:668–678
33. Geerlings P, De Proft F, Langenaeker W (2003) Conceptual density functional theory. Chem Rev 103:1793–1874
34. Yang W, Mortier WJ (1986) The use of global and local molecular parameters for the analysis of the gas-phase basicity of amines. J Am Chem Soc 108:5708–5711
35. Yang W, Parr RG (1985) Hardness, softness, and the fukui function in the electronic theory of metals and catalysis. Proc Natl Acad Sci 82:6723–6726
36. Fuentealba P, Reyes O (1993) Atomic softness and the electric dipole polarizability. J Mol Struct Theochem 282:65–70
37. De Proft F, Martin JM, Geerlings P (1996) Calculation of molecular electrostatic potentials and Fukui functions using density functional methods. Chem Phys Lett 256:400–408
38. Obot IB, Obi-Egbedi NO (2011) Anti-corrosive properties of xanthone on mild steel corrosion in sulphuric acid: experimental and theoretical investigations. Curr Appl Phys 11:382–392
39. Hassanov R, Sadıkoğlu M, Bilgiç S (2007) Electrochemical and quantum chemical studies of some Schiff base on the corrosion of steel in H_2SO_4 solution. Appl Surf Sci 253:3913–3921
40. Abboud Y, Abourriche A, Saffaj T, Berrada M, Charrouf M, Bennamara A, Hannache H (2009) A novel azo dye, 8-quinolinol-5-azoantipyrine as corrosion inhibitor for mild steel in acidic media. Desalination 237:175–189
41. Muthukrishnan P, Kumar KS, Jeyaprabha B, Prakash P (2014) Anticorrosive activity of *Kigelia pinnata* leaves extract on mild steel in acidic media. Metall Mater Trans A 45:4510–4524
42. Yadav DK, Quraishi MA (2012) Application of some condensed uracils as corrosion inhibitors for mild steel: gravimetric, electrochemical, surface morphological, UV-visible, and theoretical investigations. Ind Eng Chem Res 51:14966–14979
43. Oguzie EE, Enenbeaku CK, Akalezi CO, Okoro SC, Ayuk AA, Ejike EN (2010) Adsorption and corrosion-inhibiting effect of *Dacryodis edulis* extract on low-carbon-steel corrosion in acidic media. J Colloid Interface Sci 349:283–292
44. Da Silva AB, D'Elia E, Gomes JA (2010) Carbon steel corrosion inhibition in hydrochloric acid solution using a reduced Schiff base of ethylenediamine. Corros Sci 52:788–793
45. Avci G (2008) Corrosion inhibition of indole-3-acetic acid on mild steel in 0.5 M HCl. Colloids Surf A 317:730–736
46. Bentiss F, Bouaniss M, Mernari B, Traisnel M, Lagrenee M (2002) Effect of iodide ions on corrosion inhibition of mild steel by 3,5-bis(4-methylthiophenyl)-4H-1,2,4-triazole in sulfuric acid solution. J Appl Elechtrochem 32:671–678
47. Heusler KE, Cartledge GH (1961) The influence of iodide ions and carbon monoxide on the anodic dissolution of active iron. J Electrochem Soc 108:732–740
48. Bartos M, Hackerman N (1992) A study of inhibition action of Propargyl alcohol during anodic dissolution of iron in hydrochloric acid. J Electrochem Soc 139:3428–3433
49. Bayol E, Kayakırılmaz K, Erbil M (2007) The inhibitive effect of hexamethylenetetramine on the acid corrosion of steel. Mater Chem Phys 104:74–82
50. El Mehdi B, Mernari B, Traisnel M, Bentiss F, Lagrenée N (2003) Synthesis and comparative study of the inhibitive effect of some new triazole derivatives towards corrosion of mild steel in hydrochloric acid solution. Mater Chem Phys 77:489–496
51. Lorentz WJ, Mansfeld F (1986) Interface and interphase corrosion inhibition. Electrochim Acta 31:467–476
52. Pradeep Kumar CB, Mohana KN, Muralidhara HB (2015) Electrochemical and thermodynamic studies to evaluate the inhibition effect of synthesized piperidine derivatives on the corrosion of mild steel in acidic medium. Ionics 21:263–281
53. Benahmed M, Djeddi N, Akkal S, Laouar H (2016) Saccocalyx satureioides as corrosion inhibitor for carbon steel in acid solution. Int J Ind Chem 7:109–120
54. Bobina M, Kellenberger A, Millet JP, Muntean C, Vaszilcsin N (2013) Corrosion resistance of carbon steel in weak acid solutions in the presence of L-histidine as corrosion inhibitor. Corros Sci 69:389–395
55. Lebrini M, Robert F, Lecante A, Roos C (2011) Corrosion inhibition of C38 steel in 1 M hydrochloric acid medium by alkaloids extract from Oxandra asbeckii plant. Corros Sci 53:687–695
56. Djeddi N, Benahmed M, Akkal S, Laouer H, Makhloufi E, Gherraf N (2015) Study on methylene dichloride and butanolic extracts of *Reutera lutea* (Desf.) Maire (Apiaceae) as effective corrosion inhibitions for carbon steel in HCl solution. Res Chem Intermed 41:4595–4616
57. Li XH, Deng SD, Fu H (2010) Inhibition by *Jasminum nudiflorum* Lindl leaves extract of the corrosion of cold rolled steel in hydrochloric acid solution. J Appl Electrochem 40:1641–1649
58. Behpour M, Ghoreishi SM, Khayatkashani M, Soltani N (2012) Green approach to corrosion inhibition of mild steel in tow acidic solutions by the extracts of Punicagranatum peel main constituents. Mater Chem Phys 131:621–633
59. Deng S, Li X (2012) Inhibition by Ginkgo leaves extract of the corrosion of steel in HCl and H2SO4 solutions. Corros Sci 55:404–415
60. Quraishi MA, Sudheer Ebenso E (2012) Ketorol: new and effective corrosion inhibitor for mild steel in hydrochloric acid solution. Int J Electrochem Sci 7:9920–9932
61. Fiala A, Mechehoud Y (2012) Etude de l'effet inhibiteur du 2-(1,3-dithietan-2-ylidene)-3-oxobutanoate de méthyle et du 2-(1,3-dithiolan-2-ylidene)-3-oxobutanoate de méthyle sur la corrosion du cuivre en milieu nitrique 3 mol L^{-1}. Sci Technol A 35:23–30
62. Patel Niketan S, Snita Dalimil (2014) Ethanol extracts of Hemidesmus indicus leaves as eco-friendly inhibitor of mild steel corrosion in H_2SO_4 medium. Chem Pap 68:1747–1754
63. Zarrouk A, Hammouti B, Lakhlifi T, Traisnel M, Vezin H, Bentiss F (2015) New 1H-pyrrole-2,5-dione derivatives as efficient organic inhibitors of carbon steel corrosion in hydrochloric acid medium: electrochemical, XPS and DFT studies. Corros Sci 90:572–584

64. Li X, Deng S, Fu H (2012) Inhibition of the corrosion of steel in HCl, H_2SO_4 solutions by bamboo leaf extract. Corros Sci 62:163–175
65. Ostovari A, Hoseinieh SM, Peikari M, Shadizadeh SR, Hashemi SJ (2009) Corrosion inhibition of mild steel in 1 M HCl solution by henna extract: a comparative study of the inhibition by henna and its constituents (Lawsone, Gallic acid, α-D-Glucose and tannic acid). Corros Sci 51:1935–1949
66. Bentiss F, Lebrini M, Lagrenee M (2005) Thermodynamic characterization of metal dissolution and inhibitor adsorption process in mild steel/2,5-bis(n-thienyl)1,3,4-thiadiazoles/hydrochloric acid system. Corros Sci 47:2915–2931
67. Daoud D, Douadi T, Hamani H, Chafaa S, Al-Nouaimi M (2015) Corrosion inhibition of mild steel by two new S-heterocyclic compounds in 1 M HCl: experimental and computational study. Corros Sci 94:21–37
68. Mertens SF, Xhoffer C, De Cooman BC, Temmerman E (1997) Short-term deterioration of polymer-coated 55% Al-Zn-Part 1: behavior of thin polymer films. Corrosion 53:381–388
69. Pitchaipillai M, Raj K, Balasubramanian J, Periakaruppan P (2014) Benevolent behavior of *Kleinia grandiflora* leaf extract as a green corrosion inhibitor for mild steel in sulfuric acid solution. Int J Min Met Mater 21:1083–1095
70. Lv TM, Zhu SH, Guo L, Zhang ST (2015) Experimental and theoretical investigation of indole as a corrosion inhibitor for mild steel in sulfuric acid solution. Res Chem Intermed 41:7073–7093
71. Hegazy MA, Abdallah M, Awad MK, Rezk M (2014) Three novel di-quaternary ammonium salts as corrosion inhibitors for API X65 steel pipeline in acidic solution. Part I: experimental results. Corros Sci 81:54–64
72. Umoren SA, Obot IB (2008) Polyvinylpyrollidone and polyacrylamide as corrosion inhibitors for mild steel in acidic medium. Surf Rev Lett 15:277–286
73. Ebenso EE (2003) Synergistic effect of halide ions on the corrosion inhibition of aluminium in H_2SO_4 using 2-acetylphenothiazine. Mater Chem Phys 79:58–70
74. Singh MR, Bhrara K, Singh G (2008) The inhibitory effect of diethanolamine on corrosion of mild steel in 0.5 M sulphuric acidic medium. Portugaliae Electrochimica Acta 26:479–492
75. Obot IB, Obi-Egbedi NO (2008) Inhibitory effect and adsorption characteristics of 2,3-diaminonaphthalene at aluminum/hydrochloric acid interface: experimental and theoretical study. Surf Rev Lett 15:903–910
76. Al-Fakih AM, Aziz M, Sirat HM (2015) Turmeric and ginger as green inhibitors of mild steel corrosion in acidic medium. J Mater Environ Sci 6:1480–1487
77. Fouda AS, Al-Sarawy AA, El-Katori EE (2006) Pyrazolone derivatives as corrosion inhibitors for C-steel HCl solution. Desalination 201:1–13
78. Sultan AA, Ateeq AA, Khaled NI, Taher MK, Khalaf MN (2014) Study of some natural products as eco – friendly corrosion inhibitor for mild steel in 1.0 M HCl solution. J Mater Environ Sci 5:498–503
79. Solmaze R, Kardas G, Yazici B, Erbil M (2008) Adsorption and corrosion inhibitive properties of 2-amino-5-mercapto-1,3,4-thiadiazole on mild steel in hydrochloric acid media. Colloids Surf A Physicochem Eng Asp 312:7–17
80. Lagrenée M, Mernari B, Bouanis M, Traisnel M, Bentiss F (2002) Study of the mechanism and inhibiting efficiency of 3,5-bis(4-methylthiophenyl)-4H-1,2,4-triazole on mild steel corrosion in acidic media. Corros Sci 44:573–588
81. Behpour M, Ghoreishi SM, Soltani N, Salvati-Niasari M, Hamadanian M, Gandomi A (2008) Electrochemical and theoretical investigation on the corrosion inhibition of mild steel by thiosalicylaldehyde derivatives in hydrochloric acid solution. Corros Sci 50:2172–2181
82. Likhanova NV, Domínguez-Aguilar MA, Olivares-Xometl O, Nava-Entzana N, Arce E, Dorantes H (2010) The effect of ionic liquids with imidazolium and pyridinium cations on the corrosion inhibition of mild steel in acidic environment. Corros Sci 52:2088–2097
83. Zhang D, Li L, Cao L, Yang N, Huang C (2001) Studies of corrosion inhibitors for zinc–manganese batteries: quinoline quaternary ammonium phenolates. Corros Sci 43:1627–1636
84. Haque J, Srivastava V, Verma C, Quraishi MA (2017) Experimental and quantum chemical analysis of 2-amino-3-((4-((S)-2-amino-2-carboxyethyl)-1H-imidazol-2-yl)thio) propionic acid as new and green corrosion inhibitor for mild steel in 1 M hydrochloric acid solution. J Mol Liq 225:848–855
85. Verma C, Ebenso EE, Vishal Y, Quraishi MA (2016) Dendrimers: a new class of corrosion inhibitors for mild steel in 1 M HCl: experimental and quantum chemical studies. J Mol Liq 224:1282–1293
86. Verma C, Quraishi MA, Singh A (2016) A thermodynamical, electrochemical, theoretical and surface investigation of diheteroaryl thioethers as effective corrosion inhibitors for mild steel in 1 M HCl. J Taiwan Ins Chem Eng 58:127–140
87. Antonijevic MM, Petrovic MB (2008) Copper Corrosion Inhibitors. A review. Int J Electrochem Sci 3:1–28
88. Costa JM, Lluch JM (1984) The use of quantum mechanics calculations for the study of corrosion inhibitors. Corros Sci 24:924–993
89. Breneman CM, Wiberg KB (1990) Determining atom-centered monopoles from molecular electrostatic potentials. The need for high sampling density in formamide conformational analysis. J Comput Chem 11:176–179